Published in final edited form as:
Mol Microbiol. 2011 June ; 80(6): 1581–1597. doi:10.1111/j.1365-2958.2011.07667.x.

Sortase Independent and Dependent Systems for Acquisition of Haem and Haemoglobin in *Listeria monocytogenes*

Qiaobin Xiao[¤,§], **Xiaoxu Jiang**[¤,¶,§], **Kyle J. Moore**[¤], **Yi Shao**[¤], **Hualiang Pi**[¤], **Iharilalao Dubail**[£,¥], **Alain Charbit**[£,¥], **Salete M. Newton**[¤,¶], and **Phillip E. Klebba**[¤,¶,‡]

[¤]Department of Chemistry and Biochemistry, University of Oklahoma, Norman, OK, 73019, USA

[£]Université Paris Descartes, Faculté de Médecine, Necker-Enfants Malades, Paris, FRANCE

[¥]INSERM, U1002, Unité de Pathogénie des Infections Systémiques, Paris, FRANCE

Summary

We studied three Fur-regulated systems of *Listeria monocytogenes*: the *srtB* region, that encodes sortase-anchored proteins and a putative ABC transporter, and the *fhu* and *hup* operons, that produce putative ABC transporters for ferric hydroxamates and haemin (Hn)/haemoglobin (Hb), respectively. Deletion of *lmo2185* in the *srtB* region reduced listerial [^{59}Fe]-Hn transport, and purified Lmo2185 bound [^{59}Fe]-Hn (K_D = 12 nM), leading to its designation as a Hn/Hb binding protein (*hbp2).* Purified Hbp2 also acted as a hemophore, capturing and supplying Hn from the environment. Nevertheless, Hbp2 only functioned in [^{59}Fe]-Hn transport at external concentrations less than 10 nM: at higher Hn levels its uptake occurred with equivalent affinity and rate without Hbp2. Similarly, deletion of sortase A had no effect on ferric siderophore or Hn/Hb transport at any concentration, and the srtA-independence of listerial Hn/Hb uptake distinguished it from comparable systems of *Staphylococcus aureus.* In the cytoplasmic membrane, the Hup transporter was specific for Hn: its lipoprotein (HupD) only showed high affinity for the iron porphyrin (K_D = 26 nM). Conversely, the FhuD lipoprotein encoded by the *fhu* operon had broad specificity: it bound both ferric siderophores and Hn, with the highest affinity for ferrioxamine B (K_D = 123 nM). Deletions of Hup permease components *hupD*, *hupG*, or *hupDGC* reduced Hn/Hb uptake, and complementation of *ΔhupC* and *ΔhupG* by chromosomal integration of *hupC*$^+$ and *hupG*$^+$ alleles on pPL2 restored growth promotion by Hn/Hb. However, *ΔhupDGC* did not completely eliminate [^{59}Fe]-Hn transport, implying the existence of another cytoplasmic membrane Hn transporter. The overall K_M of Hn uptake by wild-type strain EGD-e was 1 nM, and it occurred at similar rates (V_{max} = 23 pMol/10^9 cells/min) to those of ferric siderophore transporters. In the *ΔhupDBGC* strain uptake occurred at a 3-fold lower rate (V_{max} = 7 pMol/10^9 cells/min). The results show that at low (< 50 nM) levels of Hn, SrtB-dependent peptidoglycan-anchored proteins (e.g., Hbp2) bind the porphyrin, and HupDGC or another transporter completes its uptake into the cytoplasm. However, at higher concentrations Hn uptake is SrtB-independent: peptidoglycan-anchored binding proteins are dispensable because HupDGC directly absorbs and internalizes Hn. Finally, *ΔhupDGC* increased the LD_{50} of *L. monocytogenes* 100-fold in the mouse infection model, reiterating the importance of this system in listerial virulence.

Iron, the second-most abundant metal in the Earth's crust, precipitates in water as an oxyhydroxide polymer, resulting in poor bio-availability (Neilands, 1974). Despite the paucity of soluble iron in solution, it is usually essential to pro- and eukaryotes from its

[‡]Address correspondence to peklebba@ou.edu, Tel: 405-325-4969; Fax: 405-325-6111.
[¶]current address: Department of Physiology David Geffen School of Medicine University of California Los Angeles, CA 90095
[§]Equally contributed to this work

activities as an oxygen carrier and metabolic or redox cofactor. Animals, plants and microbes compete for iron, and successful pathogens obtain it in the host environment. The majority of mammalian iron exists as haem (Hn) in myoglobin and haemoglobin (Hb), but in aerobic organisms iron functions in energy generation as an electron transfer chain cofactor, in lipid, steroid, xenobiotic and drug oxidation by cytochrome P450s, and in antioxidant defense mechanisms involving superoxide dismutases. Free Hn is toxic at excessive concentrations (Immenschuh *et al.*, 2010, Reeder, 2010, Robinson *et al.*, 2009) and bacteria regulate its accumulation (Stauff & Skaar, 2009). The upshot is that the multiple iron-containing systems of animals and bacteria lead to delicately balanced adversarial mechanisms for iron sequestration by the former (iron-binding proteins like ferritin, transferrin, lactoferrin, lipocalin), and iron acquisition by the latter organisms (siderophores and membrane iron/Hn transporters; Arslan *et al.*, 2009, Braun, 2005, Konopka *et al.*, 1982, Konopka *et al.*, 1981, Singh *et al.*, 2009, Tidmarsh *et al.*, 1983).

Bacteria produce membrane transport systems for Hn utilization during infections of animal hosts. In Gram-negative cells TonB-dependent outer membrane receptors, periplasmic binding proteins and ABC transporters capture Hn and concentrate it intracellularly (Perry *et al.*, 2003, Schneider & Paoli, 2005, Wyckoff *et al.*, 2004, Zhao *et al.*, 2010). ATP hydrolysis energizes Hn transport through the inner membrane (IM) (Burkhard & Wilks, 2008, Stojiljkovic & Hantke, 1994, Thompson *et al.*, 1999, Tong & Guo, 2007). In Gram-positive cells ABC transporters for Hn (Drazek *et al.*, 2000, Skaar *et al.*, 2004, Jin *et al.*, 2005) underlie an extensive, loosely crosslinked peptidoglycan (PG) layer, that permits diffusion of small solutes through its 20–70 Å diameter pores (Demchick & Koch, 1996, Meroueh *et al.*, 2006, Touhami *et al.*, 2004). Ferric siderophores like ferrioxamine B (FxB) and ferrichrome (Fc) need not interact with PG or proteins anchored to it: CM-resident ABC transporters are their only membrane uptake component (Jin *et al.*, 2005). The different architecture of the Gram-positive bacterial cell wall makes the pathway of Hn uptake less certain, but sortase-anchored proteins in the PG matrix extract the porphyrin from iron-containing proteins like Hb by a cascade of binding reactions that ultimately deliver it to a CM transporter (Lei *et al.*, 2003, Lei *et al.*, 2002, Nygaard *et al.*, 2006, Ran *et al.*, 2010, Zhu *et al.*, 2008).

Hn/Hb transporters exist in *Staphylococcus aureus* (Grigg *et al.*, 2010), *Streptococcus pyogenes* (Lei *et al.*, 2002), *Bacillis anthracis* (Tarlovsky *et al.*, 2010) and *Listeria monocytogenes* (Jin *et al.*, 2005), that contribute to bacterial virulence (Braun, 2005, Carniel, 2001, Stork *et al.*, 2004, Jin *et al.*, 2005). In *S. aureus* the *isd* gene cluster encodes sortase B (SrtB), an SrtB-anchored Hn binding protein (IsdC), an ABC transporter and other sortase A-dependent PG-anchored proteins (Mazmanian *et al.*, 2003). *L. monocytogenes* has a comparable *srtB*-containing genetic system, but deletion of its components, including the IsdC homolog Lmo2185, did not influence Hn/Hb uptake (Jin *et al.*, 2005). Nor did *Δlmo2185* or *Δlmo2186* (Fig. 1) reduce the virulence of *L. monocytogenes* in a mouse model (Jin *et al.*, 2005). Rather, iron acquisition from both the porphyrin and the protein required the activity of the putative ABC-transporter encoded by the *hup* chromosomal region (2498.3 – 2501.1 kb); *ΔhupC* impaired Hn and Hb uptake and decreased virulence (Jin *et al.*, 2005).

Because of uncertainties in the Gram-positive bacterial Hn transport pathway we further studied its uptake by *L. monocytogenes*. The putative Hn binding protein, HupD, displayed selectivity for the iron porphyrin, which contrasted the behavior of the ferric hydroxamate binding protein, FhuD, that showed broad recognition of numerous ferric siderophores. These data, and the impairment of Hn/Hb uptake by deletion of *hupG* (*lmo2430*), *hupD* (*lmo2431*)] or the whole operon (*Δhup*) reiterated the specificity of the Hup membrane permease. High sensitivity [^{59}Fe]-Hn uptake assays defined the kinetic properties of the

HupDGC transporter, identified a second Hn/Hb uptake system in *L. monocytogenes*, and showed a role for SrtB-anchored Lmo2185 in capture of the iron porphyrin. Sortase A - deficient bacteria, on the other hand, showed no defects in Hn/Hb acquisition.

Results

Specificities of the FhuD and HupD binding lipoproteins

In *L. monocytogenes* the Fur-regulated (Baichoo *et al*, 2001) *fhu* and *hup* operons (Fig. 1) contain genes for binding proteins (*fhuD, hupD*), membrane permeases (*fhuB, fhuG, hupG*), and ATPase components (*fhuC, hupC*) of putative ABC transporters that function in the acquisition of ferric hydroxamate siderophores and Hn/Hb, respectively (Jin *et al.*, 2005). To define the selectivities of the two systems we cloned, overexpressed and purified their binding proteins, and then assayed their adsorption of ferric siderophores and porphyrins. Although neither listerial protein is structurally solved, both are related to *E. coli* FhuD [EcoFhuD; PDB 1ESZ (Clarke *et al.*, 2002)]: LmoFhuD is 19% identical and 59% similar; LmoHupD is 17% identical and 57% similar. All three binding proteins contain Trp: LmoFhuD at residues 158, 229 and 271, LmoHupD at residue 280, and EcoFhuD at residues 43, 68, 102, 210, 217, 255 and 273. EcoFhuD W273, situated in the solute binding site, aligns with W271 in LmoFhuD and and W280 in LmoHupD.

Trp in proximity to the binding cavity permitted fluorescence spectroscopic measurements of ligand adsorption to purified *L. monocytogenes* 6H-FhuD and 6H-HupD. These data (Fig. 2; Table 1) revealed a hierarchy of multispecificity in the former protein. It had the highest affinity for FxB (K_D = 0.1 uM), with lower affinities for other ferric hydroxamate siderophores [FcA (K_D = 0.4 uM), Fc (K_D = 0.5 uM)]. But, 6H-FhuD also bound porphyrins [PPIX (K_D = 0.3 uM), Hn (K_D = 0.7 uM)], and even FeEnt (K_D = 3.1 uM), which is structurally distinct from the hydroxamates or porphyrins. The ferric catecholate caused less quenching, suggesting its incomplete occupancy of the binding site. We conducted the initial measurements of these binding reactions with purified proteins that retained an N-terminal 6-His tag (Fig. 2), but because hexahistidine may coordinate Fe^{++} (e.g., at the iron center of Hn), we also assayed purified FhuD from which the 6-His sequence was proteolytically removed. The hexahistidine tag had no effect on measured affinities for ferric siderophores and Hn (Table 1).

In contrast to LmoFhuD, the high affinity and specificity of 6H-HupD for Hn was apparent even during its purification. When expressed in *E. coli* DH5α and purified by Ni^{++}-NTA chromatography, solutions of 6H-HupD were yellow, red or brown, and their visible spectra showed Soret peaks characteristic of Hn. Removal of the bound iron porphyrin from 6H-HupD required either anion exchange chromatography or SDS-denaturation of the protein. Unlike FhuD, purified 6H-HupD was virtually monospecific: it bound Hn with 5-fold higher affinity (K_D = 26 nM) than the most avid LmoFhuD binding interaction, and did not measurably adsorb the other iron complexes that we tested. Only PPIX also bound to LmoHupD, but with 40-fold lower affinity, indicating the importance of iron in the recognition reaction. Again, proteolytic removal of the 6H tag did not significantly alter the affinity of HupD for Hn (Table 1). In summary, the two binding proteins of the ABC transporter systems were different: the former had lower affinity and broad specificity for ferric siderophores, whereas the latter manifested high affinity and monospecificity for the iron porphyrin.

Effects of *hup* operon deletions on growth of *L. monocytogenes* in iron-deficient media

L. monocytogenes does not utilize the complex of Fe^{+++} and 2, 2'-bipyridyl (BP) as an iron source (Jin *et al.*, 2005, Newton *et al.*, 2005), so we employed BP to render the bacteria

iron-deficient in microbiological media. In BHI media inoculated with the wild type strain (EGD-e) or its mutant derivatives the addition of 1 mM BP inhibited growth, but when 0.2 mM Hn was added EGD-e returned to its original growth rate and ultimately reached a higher density. However, otherwise isogenic strains with *ΔhupC*, *ΔhupG* or a complete, precise deletion of the entire *hup* operon (*ΔhupDGC*) were not stimulated by Hn, unless we complemented the chromosomal deletions by introduction of the corresponding wild-type gene (*ΔhupC*/hupC$^+$ and ΔhupG/hupG$^+$; Fig. 3). These findings reiterated the specificity of the *hup* operon: *ΔhupC*, *ΔhupG* and *ΔhupDGC* impaired Hn capture, while chromosomal reinstatement of those genes restored it.

We also assessed the ability of mutant strains to utilize Hn by microbiological nutrition tests (Newton *et al.*, 2005, Wayne *et al.*, 1976). In a previous study only relatively high concentrations of Hn [200 uM; (Jin *et al.*, 2005)] stimulated the growth of EGD-e, and we found that the low sensitivity derived from poor solubility of Hn in aqueous buffers. Hn may dimerize and precipitate in aqueous solution (Collier *et al.*, 1979, de Villiers *et al.*, 2007, Asher *et al*, 2009), but a solvent/buffer system containing DMSO (Experimental Procedures) minimized formation of the π-π and/or μ-oxo-dimers, improving its solubility. When stored in DMSO stocks and diluted into media, Hn stimulated growth at concentrations as low as 0.5 uM. Under these conditions, deletions in the *hup* operon (*ΔhupC*, Δ*hupD*, *ΔhupG* or *ΔhupDGC*) decreased or eliminated Hn (and Hb) uptake (Fig. 4). The iron nutrition tests showed greater impact from loss of the membrane permease (HupG) than loss of the ATPase component (HupC), in that the *ΔhupG* strain did not respond to Hn or Hb at 5 uM, but the *ΔhupC* mutant showed a faint halo around that concentration. This result may derive from the ability of ATPase components of different ABC transporters to substitute for each other. Complementation of *ΔhupC* and *ΔhupG* by integration of pPL2 vectors (Lauer *et al.*, 2002) carrying their corresponding wild type genes restored Hn/Hb uptake. However, our attempted complementation of Δ*hupD* was unsuccessful, even though the pPL2*hupD*$^+$ integrated into the chromosome of the *hupD* deletion mutant. We also attempted complementation when pPL2*hupD*$^+$ contained the stronger *clpB* promoter (Chastanet *et al.*, 2004), but again without success. *hupD* is the first gene in the operon, and its deletion may cause a polar effect on downstream genes.

Among listerial sortase mutants, nutrition tests did not show an effect of *ΔsrtA* on Hn or Hb uptake. These and other data (see following) indicated that SrtA-anchored proteins have no obvious role in ferric siderophore or Hn/Hb acquisition. On the other hand, SrtB anchors the product of *lmo2185* (formerly known as SvpA) to PG. The improved-sensitivity Hn nutrition assay showed that *Δlmo2185* reduced uptake of Hn at 0.5 and 5 uM; at 50 uM Hn the strain behaved like EGD-e (Fig. 4a). Furthermore, Lmo2185 bound Hn (Jin *et al.*, 2005; see below), and it promoted growth of *L. monocytogenes* EGD-e in iron nutrition tests (Fig. 4b), demonstrating its activity as a hemophore (Arnoux *et al.*, 1999). However, both apo- and holo- Lmo2185 were inactive or barely stimulatory to a *Δlmo2185* strain, suggesting that Hn uptake by this route requires the SrtB-anchored form of the cell envelope protein.

Hn binding and transport

We synthesized [^{59}Fe]-Hn (Experimental Procedures) and measured its binding and uptake by EGD-e and derivatives with deletions in the *hup* operon (Table 2, Fig. 5), again using conditions to avoid rapid formation of Hn dimers. When grown in MOPS-L (Experimental Procedures) the binding capacity of EGD-e for [^{59}Fe]-Hn was 130 pmol/10^{9}cells and the K_D of the binding interaction was 2.4 nM. Complete deletion of the *hup* operon did not eliminate Hn adsorption, but decreased binding capacity by ~20%, to 105 pmol/10^{9}cells. Further experiments ascribed the residual Hn binding to two systems: an additional cytoplasmic membrane transporter, and to sortase B-anchored proteins in the cell wall (see below).

Again, the *ΔsrtA* strain lacked a phenotype in Hn binding studies. It absorbed [^{59}Fe]-Hn with roughly the same affinity and precisely the same capacity as EGD-e. We saw a slight (2-fold) difference in [^{59}Fe]-Hn binding capacity between the *ΔsrtB* (19 pMol/10^9 cells) and *ΔsrtAB* (9 pMol/10^9 cells) strains. But, when compared to the ~10-fold higher capacity of both EGD-e and the *ΔsrtA* mutant (130 pMol/10^9 cells) the significance of this variation was questionable, and complicated by the error inherent in measurements of weak residual binding by the *ΔsrtB* strain. Thus, sortase A had no impact on Hn binding, and the *ΔsrtB* mutation decreased the Hn binding capacity in the double mutant.

[^{59}Fe]-Hn uptake studies showed the presence of a second Hn transporter. For EGD-e the V_{max} of [^{59}Fe]-Hn uptake was 23 pMol/10^9 cells and its overall uptake K_M was ~1 nM. In a *ΔhupDGC* strain [^{59}Fe]-Hn uptake persisted, but V_{max} decreased to 7.5 pMol/10^9 cells/min, 27% of the wild type rate (Fig. 5). Thus, Hup is not the only CM transporter for Hn in *L. monocytogenes*, and the kinetic and thermodynamic properties of the residual system are similar to those of Hup system: V_{max} was lower, but K_M was the same (~1 nM). Subtraction of the residual accumulation in *Δhup* from that of the wild-type gave an estimate of the Hup-dependent transport rate: V_{max} was 14 pMol/10^9 cells/min.

Sortase B and Lmo2185 in Hn binding and uptake

The availability of [^{59}Fe]-Hn also allowed evaluation of sortase-dependent, PG-anchored proteins in Hn transport. Lmo2185 is partly secreted into the extracellular environment, but a portion remains anchored to PG by sortase B (Newton *et al.*, 2005). The primary structures of Lmo2185 and Lmo2186 (from the same transcriptional unit) show considerable identity with the Hn binding protein SauIsdC (Fig. 6; Discussion). Hn associates with Lmo2185 (Newton *et al*, 2005), so we determined the effect of *Δlmo2185* and *ΔsrtB* on binding and transport of the iron porphyrin. The improvements in Hn solubility enhanced its activity in nutrition tests with EGD-e, but these assays still did not reveal effects of *Δlmo2185* or *ΔsrtB* on Hn uptake (Fig. 4). We only observed their impact in quantitative binding and transport experiments at lower concentrations (Fig. 5; Table 4), where *Δlmo2185* and *ΔsrtB* reduced [^{59}Fe]-Hn binding capacity and transport rate to about 20% of what was seen in EGD-e. In the same tests *ΔsrtA* did not affect [^{59}Fe]-Hn binding K_D nor capacity, nor its transport K_M nor V_{max}. The double mutant *ΔsrtA*B was indistinguishable from *ΔsrtB* alone (Table 2). Hence, in *L. monocytogenes* Hn/Hb acquisition was always *srtA* independent, but *srtB*-dependent at low concentrations.

These results agreed with the high affinity of purified Lmo2185 for Hn: in equilibrium determinations of [^{59}Fe]-Hn binding to Lmo2185 the K_D was 12 nM (Fig. 5). Furthermore, like HupD above, purified Lmo2185 contained bound Hn (at ~50% saturation), as evidenced by a Soret band (at 405 nm) in its visible spectrum and a positive pyridine haemochrome test (data not shown).

Role of the *hup* locus in virulence and intracellular multiplication of *L. monocytogenes*

We determined the infectivity of the triple deletion mutant EGD-e*ΔhupDGC* by intravenous inoculation of Swiss mice (Table 3). Its LD_{50} was $10^{6.4}$, as compared to $10^{4.5}$ for the parental strain EGD-e. These data were consistent with previous estimation of LD_{50} for the single mutant EGD-e*ΔhupC* ($10^{6.2}$; Jin *et al.* 2006). The 100-fold attenuation of virulence relative to the wild-type strain reiterated that the *hup* locus plays a role in *L. monocytogenes* pathogenesis in the mouse model.

We also monitored the intracellular multiplication of the single deletion mutants *ΔhupC*, *ΔhupG*, *ΔhupD*, and *ΔhupDGC* in bone marrow-derived macrophages (Fig. S3). None of

them showed growth defects relative to EGD-e, indicating that the *hup* loci do not affect intracellular survival of *L. monocytogenes*.

Discussion

The comparative biochemistry of iron uptake through the Gram-positive and Gram-negative cell envelopes is a question of interest. Toward that end we quantitatively characterized, for the first time, the membrane Hn/Hb acquisition systems of *L. monocytogenes*. In the wild type strain the uptake process was similar to ferric siderophore transport. The steady-state Hn uptake rate was nearly identical to that of the listerial CM Fc transporter (FhuDBGC: V_{max} = 22 pMol/10^9 cells/min; Jin *et al.*, 2005), which is approximately half the rate of enteric bacterial Fc transport (*E. coli* FhuA: V_{max}= 45 pMol/10^9 cells/min; Newton *et al.*, 2010). The main distinction of listerial iron acquisition was lower overall affinity. For Hn or Fc transport, $K_D \approx K_M \approx 1$ nM, 10-fold lower affinity than that of ferric siderophore transport systems of *E. coli* [for ferric enterobactin or Fc, $K_D \approx K_M \approx 0.1$ nM (Newton *et al.*, 1999, Scott *et al.*, 2001, Annamalai *et al.*, 2004)].

Gram-negative bacteria initiate iron uptake with tight binding of metal complexes to the external surfaces of the OM proteins that transport them. Despite their lack of an OM, Grampositive cells also produce high-affinity cell surface binding sites for adsorption of eukaryotic haemoproteins (Lei *et al.*, 2002, 2003; Mazmanian *et al.*, 2002, 2003). The physiological role of Lmo2185 in iron transport was in doubt, but several of our findings showed that the sortase B-anchored protein binds Hn with high affinity. Sequence homologies in the context of the staphylococcal IsdC crystal structure revealed its relatedness to Lmo2185 and Lmo2186 (Fig. 6). The three proteins contain sufficient sequence identity to assure their structural similarity (Ginalski, 2006, Kryshtafovych *et al.*, 2005), and the conservation of IsdC Hn-binding residues in Lmo2185/6 agrees with the high affinity of purified Lmo2185 for [^{59}Fe]-Hn. Therefore, we propose to rename Lmo2186 as Hbp1 (Hn/Hb binding protein), and Lmo2185, which duplicates Lmo2186 (Fig. 6), as Hbp2.

In the *srtB* locus of *L. monocytogenes*, *hbp1* and *hbp2* encode IsdC homologs with NPKSS and NAKTN sorting motifs, respectively (Bierne, 2004). Synthesis of both proteins is Fur-regulated and they are over-produced in iron-deficient environments. The post-secretion fate of the former is unknown, whereas 10–50% of Hbp2 is anchored to PG, depending on growth conditions (Newton *et al.*, 2005). In the nanomolar concentration range of [^{59}Fe]-Hn, *ΔsrtB* and *Δhbp2* decreased its binding capacity 80% (from 130 pMol/10^9 cell to 30 pMol/10^9 cells), while *Δhup* only dropped it 20% (to 105 pMol/10^9 cells). Therefore, at low external concentrations Hbp2 is the primary Hn adsorption site, and Hup accounts for the remainder. Hup is 4-fold less abundant than Hbp2, as estimated by [^{59}Fe]-Hn binding capacities, immunoblots (data not shown) and proteomics data (Ledala *et al.*, 2010). Secondly, besides being the predominant Hn binding constituent, Hbp2 has the highest affinity for it. Measurements of whole cell affinity for [^{59}Fe]-Hn (K_D = 2 nM) were comparable to those of purified Hbp2 (K_D = 12 nM), and *Δhbp2* caused a 5-fold reduction in Hn binding affinity (K_D to ~10 nM), while *Δhup* caused no observable change. [^{59}Fe]-Hn uptake results agreed with the binding data: *ΔsrtB* and *Δhbp2* decreased the uptake rate 80% or more, and reduced overall uptake affinity 5–10 fold (*Δhbp2* resulted in a non-saturable uptake process). These data show that at concentrations < 50 nM Hn acquisition is SrtB-dependent in *L. monocytogenes*, as proposed in *S. aureus* (Maresso *et al.*, 2006, Mazmanian *et al.*, 2003). Still, in radioisotopic tests neither Hbp nor SrtB affected uptake above this 50 nM threshold, so in environments containing more Hn the iron complex directly interacts with its CM transporter(s). *L. monocytogenes* is β-hemolytic, and proteolytic degradation of haemoglobin at sites of infection or abscess will result in release of free haemin.

In Gram-positive bacteria sortase-anchored proteins bind Hb in the PG framework (Maresso *et al.*, 2006, Mazmanian *et al.*, 2003), presumably facilitating the subsequent extraction of Hn for delivery to CM transporters. The family of known and putative Gram positive bacterial haem binding proteins (Table 4) has considerable sequence and structural variability. Among the secreted or PG-(sortase)anchored binding proteins, Hbp1 and Hbp2 of *L. monocytogenes*, IsdC, IsdX1 and IsdX2 of B. anthracis, and IsdC of *S. aureus* form a subfamily. Hbp1, IsdC and IsdX all contain the same 8-stranded β -barrel nucleus (Fig. 6); Hpb2 and IsdX2 duplicate this domain, linked by an intervening polypeptide of ~200 and 370 a.a., respectively. With the exception of IsdX1, all these proteins contain potential SrtB cleavage sites (NPXZN). However, IsdX1, IsdX2 (Maresso *et al.*, 2008; Fabian *et al.*, 2009) and a large fraction of Hbp2 (Newton *et al.*, 2005) are secreted to the environment, where the three proteins act as hemophores (Fabian *et al.*, 2009; this report). The streptococcal proteins Shp (Lei *et al.*, 2002) and Shr (Zhu *et al.*, 2008) are unique among the group: the former has a different structural format than the other heme-binders, and unexpectedly, the latter shows the most relatedness to InlA (20% identity). From their sequence relatedness and SrtA-mediated attachment to PG, the staphylococcal proteins IsdA, IsdB and IsdH form another subfamily of heme binding proteins. IsdB, IsdH and IsdA are proposed to bind Hb, extract Hn and transfer it to SrtB-dependent IsdC, which passes the porphyrin to the CM ABC transporters IsdDEF or HtsABC (Mazmanian *et al.*, 2002, 2003, Reniere *et al.*, 2007). According to this scheme the staphylococcal Hn/Hb uptake system requires sortase A-anchored proteins. Nevertheless, for *L. monocytogenes* the *ΔsrtA* mutation did not influence listerial Hn/Hb uptake in any assay, at any concentration, indicating that sortase A-anchored proteins play no role in listerial Hn acquisition.

Deletion of the *hup* operon or its individual membrane permease components decreased but did not eliminate Hn uptake, implying the existence of additional CM Hn transport systems in *L. monocytogenes*. The Hup permease is the primary CM Hn transporter, because its steady-state uptake rate is twice that of the residual system. The overall affinity of the secondary CM Hn transporter is similar to that of HupDGC. Other Gram-positive bacterial CM transporters of iron and haem are known (Table 4). Listerial FhuDBGC (Jin *et al.*, '05), staphylococcal FhuCBG (Sebulsky *et al.*, 2000) and streptococcal FtsABCD (Hanks *et al.*, 05) all transport ferric hydroxamates. Their micromolar affinites for the hydroxamate iron complexes leaves no doubt about their specificity. However, LmoFhuD was also promiscuous for other iron complexes, including Hn, raising the possibility that FhuDBGC provides an auxiliary pathway for Hn uptake. In *S. aureus* both IsdDEF and HtsABC ABC-transporters are thought to transport Hn (Skaar *et al.*, 2004); the HtsABC complex also functions in *Streptococcus pyogenes* (Liu & Lei, 2005; Nygaard *et al.*, 2006). LmoHupDGC is most closely related to SauHtsABC (24%, 26% and 46% identity, respectively, between the individual components), even though the staphylococcal *srtB* region encodes the proposed ABC-transporter IsdDEF.

The pathways of heme and hemoglobin passage through the Gram-positive cell wall, and the interactions among potential uptake components are not obvious: how do binding proteins attached within the PG matrix facilitate Hn transport through ABC-transporters as much as 50 – 100 Å away, in the cytoplasmic membrane? The answer is that at concentrations greater than 50 nM sortase-anchored proteins are not needed for Hn uptake by *L. monocytogenes*. The cell wall architecture (Fig. 6) contains pores that allow diffusion of the porphyrin to CM permeases. Thus, besides the dispensability of SrtA-anchored proteins, even SrtB-anchored proteins have a limited role in Hn uptake. They are only advantageous at very low external Hn concentrations (<50 nM), and at higher levels SrtB and Hbp are inconsequential. Corroborating this point, the cytoplasmic HupDGC membrane transporter, not the sortase-anchored proteins, was most crucial to listerial virulence. We note that LD_{50} determinations of strains containing complemented *hup* operon deletions are still needed to

complete the analysis of its contributions to pathogenesis. Furthermore, the exact role of Hup-mediated Hn/Hb uptake in bacterial infection remains mysterious. RNome analysis (which studies the structure and function of non-coding RNAs) revealed that incubation of *L. monocytogenes* in human blood up-regulates several virulence genes (Toledo-Arana *et al.*, 2009), implicating them in blood stage dissemination. HupC expression was unchanged in these conditions. *In vivo* transcriptome profiling showed increased Fur expression *in vivo* in mice [7.67-fold at 48h; (Camejo *et al.*, 2009)], but this up-regulation did not correlate with increased repression of Fur-regulated iron ABC transporters. Instead, the Fur-controlled *srtB* locus was up-regulated *in vivo*, whereas expression of the *fhuGBDC* and *hupDGC* loci did not vary. Thus, the relationship between external iron availability and Fur-regulated gene expression encompasses complex relationships and/or regulatory cascades that affect pathogenesis, but by still unknown mechanisms

Experimental Procedures

Bacterial strains, plasmids and media

(Table 5) *E. coli* strains DH5α (Dower *et al.*, 1988) or XL-1 blue (Li *et al.*, 1990) hosted the thermosensitive shuttle vector pKSV7 (Glaser *et al.*, 2001). Using this plasmid we deleted chromosomal genes of *L. monocytogenes* strain EGD-e (Jin *et al.*, 2005). Using the site-specific phage integration vector pPL2 (Lauer *et al.*, 2002) we re-introduced wild type alleles of the deleted genes into the chromosome, to verify their ability to complement the original mutations (*hupC* and *hupG*).

We selected spontaneous streptomycin-resistant clones of all the EGD-e mutant derivatives, which facilitated their growth in minimal media without contamination. Bacteria were routinely grown on plates and in broth {*E. coli*: Luria–Bertani broth (LB; Difco); *L. monocytogenes*: brain heart infusion (BHI; Difco)}. For cultivation of *L. monocytogenes* in iron-deficient conditions we use medium MOPS-L, a minimal medium that we adapted from the original MOPS formulation for Enterobacteriaecae (Neidhardt *et al.*, 1974). Because *L. monocytogenes* is more fastidious, we increased the concentration of glucose from 0.4% to 1%, and added additional micronutrients, vitamins, cysteine and glutamine (Premaratne *et al.*, 1991, Tsai & Hodgson, 2003; Table 6) To prepare the modified medium we added the following components at the indicated final concentrations to MOPS medium: Cys (0.1 mg/mL), Glu (0.6 mg/mL), casamino acids (0.1%), tryptophan (50 μg/mL), riboflavin (0.5 μg/mL), biotin (1 μg/mL), thiamine (1 μg/mL), lipoic acid (0.005 μg/mL), $(NH_4)_6Mo_7O_{24}{\cdot}4H_2O$ (3×10^{-7} M), $CoCl_2{\cdot}6H_2O$ (3×10^{-6} M), HBO_3 (4×10^{-5} M), $CuSO_4{\cdot}5H_2O$ (10^{-6} M), $MnCl_2$ (8×10^{-6} M), $ZnCl_2$ (10^{-6} M), and glucose (1%).

Site-directed deletions

We used homologous recombination to delete chromosomal genes of strain EGD-e (Bierne, 2004, Jin *et al.*, 2005, Newton *et al.*, 2005), and verified the correct structure of the resulting mutants by colony-PCR and DNA sequencing. For PCR reactions, we utilized Taq 2X mix (New England Biolabs) and oligonucleotide primers synthesized by Invitrogen. Primer sequences are listed in Table S1.

Complementation of deletions

By PCR, we amplified the 155-bp DNA fragment containing the promoter region of the *hup* operon (upstream of *lmo2432*) on the EGD-e chromosome, flanked by *BamHI* and *PstI* restriction sites. We transferred this PCR fragment into pPL2 [Cm^r; (Lauer *et al.*, 2002)] to generate pPro, and then separately cloned wild type *hupC* and *hupG* into it using the *PstI* site upstream and a *KpnI* (in the multiple cloning site) downstream. We individually transformed the resulting constructs (pHupC, pHupG) into *E. coli* SM10, and used the

resulting *E. coli* strains as donors for plasmid transfer to *L. monocytogenes ΔhupC* or *ΔhupG* (Sm^r). After mixing the strains in BHI broth and incubating for 2 hours at 37°C, we spread the mixture on BHI plates containing both antibiotics and incubated overnight. From double resistant colonies we isolated the complementation constructs and verified them by DNA sequencing.

Growth assays

EGD-e and its mutant derivatives were grown in BHI at 37 °C overnight, and 2.5×10^7 cells were subcultured (1%) into 10 mL BHI containing 1 mM 2, 2'-bipyridyl (BP), with or without Hn. We spectrophotometrically monitored the growth of the cultures at 600 nm until stationary phase.

Nutrition tests

Fc was purified from cultures of *Ustilago sphaerogena* (Emery, 1971). Hn and bovine Hb were from Sigma-Aldrich (St. Louis). *L. monocytogenes* was grown in BHI until OD_{600} 0.2, 1 mM BP was added to the culture and the cells were grown for another 3.5 hours, when 200 μL aliquots were mixed with 8 mL BHI top agar containing 0.25 mM BP and poured onto a BHI plate. Paper discs were applied to the agar surface, aliquots of solutions of Fc, Hn or bovine Hb were applied to the discs, and the plates were incubated overnight at 37°C (Jin *et al.*, 2005, Newton *et al.*, 2005).

[^{59}Fe]-Hn

We chemically synthesized [^{59}Fe]-Hn by inserting ^{59}Fe into protoporhyrin IX (PPIX) (Babusiak *et al.*, 2005). 50 μL of a solution of PPIX (Sigma-Aldrich; 6 mg/mL in pyridine) was added to 450 μL of glacial acetic acid, and maintained at 60°C under N_2 in a sealed flask. 0.25 μL of thioglycolic acid (Sigma-Aldrich) was added to a 30 μg of $^{59}FeCl_3$ (Perkin-Elmer) in 50 μL of 0.5 M HCl, and the mixture was immediately injected into the PPIX solution. After 30 min at 60°C, the solution was stirred for 1.5 hours at room temperature and then transferred to 20 mL of ethyl ether, and washed 5 times with 30 mL of 1M HCl to remove unreacted iron and porphyrin. The organic phase was dried overnight under a mild flow of nitrogen, and the dried [^{59}Fe]-Hn was stored dessicated at 4°C. Its purity was evaluated by thin layer chromatography: [^{59}Fe]-Hn in dimethyl sulfoxide (DMSO) was spotted on silica gel plate (60 F_{254}, Merck) and developed with a mixture of 2, 6-lutidine and water (5:3.5, v: v) (Falk, 1964; Fig. S1). The concentration of the [^{59}Fe]-Hn stock solution was determined by UV-VIS spectrophotometry in 40% DMSO, using a millimolar extinction coefficient of 180 $mM^{-1}cm^{-1}$ at 400 nm (Sinclair, 1999). We synthesized [^{59}Fe]-haem under reducing conditions, but upon its addition to culture media it oxidized to [^{59}Fe]-haemin. Hence, in our experiments haemin was the primary porphyrin under investigation, but these solutions contained some haem. It was not possible to analytically monitor the concentrations of the two porphyrins, or to functionally discriminate between them.

[^{59}Fe]-Hn binding experiments

We prepared and stored solutions of [^{59}Fe]-Hn in DMSO, prior to dilution into transport media and/or buffers (Collier *et al.*, 1979). We also evaluated 50 mM NaOH to maintain Hn in soluble, monomeric form. The porphyrin had good initial solubility and gave the same results in fresh in NaOH solutions as in DMSO, but it tended to dimerize over time, which we did not observe in DMSO, making it the solvent of choice. Additionally, the hydrophobicity of its porphyrin ring system promotes the adsorption of Hn to many filtration materials, and to reduce its nonspecific binding to the solid phase we added 0.05% Tween-20 to the binding and transport washing buffers. EGD-e and mutant derivatives were

grown in 20 mL BHI at 37°C overnight, subcultured (1%) in MOPS-L and grown to OD_{600nm} = 0.8, then subcultured (1%) again into 50 mL MOPS-L, shaken at 37 °C until the OD_{600nm} reached 0.6 – 0.8, and finally assayed for binding and uptake of [^{59}Fe]-Hn. Binding experiments were performed on ice. Appropriate amounts of [^{59}Fe]-Hn were added to 25 mL of ice cold MOPS-L and the mixtures were immediately poured onto 100 μL aliquots of bacterial cells in 50 mL test tubes, and incubated for 1 min before collection by filtration. The 0.45 micron Durapore filters (Millipore) were washed with 25 mL of 50 mM Tris-HCl, pH 9.0, containing 0.05% Tween-20, and counted in a Packard Cobra gamma counter. CPM from adsorption of [^{59}Fe]-Hn alone to the filters at each concentration were measured as background and subtracted from the CPM of the cell binding reactions. Data were collected in triplicate at each concentration, averaged, and K_D and binding capacity were calculated using the "Ligand Binding (1 Site + Background)" equation of Grafit 6.0 (Erithacus, Middlesex UK).

Purified Hbp2 (see below) was assayed by initially diluting it to 30.6 pmol/mL in TBS, pH 8.0, and incubating at room temperature for 1 hour to allow refolding of the protein. [^{59}Fe]-Hn was prepared at various concentrations in DMSO, and 100 uL aliquots were mixed with 4.9 mL of TBS pH 8.0, or TBS containing purified Hbp at pH 8.0. The reactions were transferred to ice and after 30 min each sample was collected on cellulose acetate filters and washed with 5 mL of TBS pH 8.0 plus 0.05% TWEEN 20. The radioactivity on each filter was measured in a Packard Cobra gamma counter. Each concentration of [^{59}Fe]-Hn was performed in triplicate and averaged. The radiation accumulated on the filters without protein present was subtracted as a background control, and the differential counts were used to determine the K_D of Hbp2 for Hn.

[^{59}Fe]-Hn uptake

L. monocytogenes strain EGD-e and its mutant derivatives were inoculated in 10 mL BHI broth at 37°C overnight. In the next morning, the stationary phase BHI culture was sub-cultured at 1% into 20 mL MOPS-L and grown to stationary phase. The full-grown MOPS-L culture was subcultured again at 1% into 20 mL of MOPS-L, and grown to an $O_{D600\ nm}$ of 0.8–1. The bacteria were then subjected to [^{59}Fe]-Hn uptake assays at 37°C: 100 uL aliquots of the cell cultures were mixed with 10 mL MOPS media pre-warmed to 37°C, containing varying concentrations of [^{59}Fe]-Hn. After incubation at 37°C for 5 seconds or 1 minute, the reaction was filtered through a 0.45 micron Durapore filter and washed with 10 mL ice cold wash buffer (50 mM Tris, 0.05% Tween-20, pH 9). The radiation on the filters was measured in a Packard Cobra gamma counter. At each concentration, data were collected in triplicate and averaged. The radiation accumulated during the 5 s time point was subtracted from that of the 1 min time point to determine the uptake rate. Transport K_M and V_{max} were calculated using the 'Enzyme Kinetics' equation of Grafit 6.0 (Erithacus, Middlesex, UK).

Purification of FhuD and HupD

For expression and purification of FhuD and HupD of *L. monocytogenes*, we cloned their structural genes into pET28a, devoid of their signal sequences (FhuD: residues 1–23; HupD: residues 1–20), and transformed the clones (p6HΔssFhuD, p6HΔssHupD) into *E. coli* BL21. The elimination of their signal sequences resulted in high-level over-expression of the two binding proteins as soluble, rather than periplasmic proteins. This strategy dramatically enhanced expression, which facilitated their Ni^{++}-NTA chromatographic purification. We grew the strains to mid-log phase (OD_{600nm} ≈0.5) in LB broth plus kanamycin, added IPTG (0.5 mM), and continued shaking the cultures at 37 °C for another 3–4 hours. The cells were pelleted by centrifugation (3000 × g, 20 min), resuspended in lysis buffer (50 mM NaH_2PO_4, 300 mM NaCl, 10 mM imidazole, pH 8.0) containing RNAse and DNAse (both at 10ug/mL), and lysed by passage through a French pressure cell at 14,000 p.s.i. The lysate

was clarified by centrifugation at 4000 g for 20 minutes, and the supernatant was centrifuged at 100,000 × g for 1 hour. The supernatant (cytoplasm) was passed through a Ni^{++}-NTA column (Qiagen) equilibrated with lysis buffer. After loading, the column was washed with 10 volumes of lysis buffer, followed by 10 volumes of 50 mM NaH_2PO_4, 300 mM NaCl, 20 mM imidazole, pH 8.0, and eluted with a linear gradient of imidazole (40–250 mM) in lysis buffer. Fractions were collected and subjected to SDS-PAGE (Fig. S2). Fractions containing purified 6H-FhuD and 6H-HupD were pooled, dialyzed against Tris-buffered saline (TBS: 150 mM NaCl, 50 mM Tris, pH 7.4), and stored frozen at −20 °C. Protein concentrations were determined by Bradford assay.

In the case of 6H-HupD, pooled fractions of the purified protein were colored, varying from light yellow to brown: the more concentrated the protein fraction, the darker its color. UV-visible spectroscopy showed absorption around 400 nm, and Soret peaks that are diagnostic of an iron porphyrin. 6H-HupD was isolated with bound Hn, and the chromophore was not removed by dialysis. To test whether the bound Hn derived from the growth medium or was synthesized by the bacteria, we purified 6H-HupD from bacteria grown in MOPS minimal medium (which does not contain any Hn), but the purified binding protein was still loaded with Hn. Thus, the porphyrin bound by 6H-HupD was synthesized by BL21 cells. To separate the Hn from the binding protein, we mixed 6H-HupD with 1% SDS, boiled the sample for 5 min and chromatographed it over Sephacryl S100 HR equilibrated in 10 mM Tris-Cl, 1% SDS, pH 8.0. 1 mL fractions were collected and spectroscopically analyzed at 280 nm and 405 nm. This method separated Hn from 6H-HupD, but left the protein in a denatured state. Nevertheless, ion exchange chromatography of the native complex also yielded the apo-protein. 6H-HupD was loaded onto DEAE Sepharose (1.5 × 50 cm) equilibrated with 10 mM, pH 8.0 Tris-Cl. After loading the column was washed with 5 volumes of buffer and eluted with a linear gradient of 0 –1M NaCl in the same buffer. Purified apo-6H-HupD was dialyzed against Tris-HCl, and spectrophotometric analyses showed that it was 98–99% free of Hn. A pyridine haemochrome test (Zhu et al, 2008) confirmed the absence of Hn in the purified apo-6H-HupD (data not shown).

The pET28a expression vector inserts thrombin cleavage site between the N-terminal 6H tag and the initial residue of cloned proteins. We also removed the hexahistidine tags from both 6H-FhuD and 6H-HupD by incubation with biotinylated thrombin (EMD Biosciences), followed by chromatography of the reaction mixture over avidin-sepharose (Fig. S2). The eluted FhuD and HupD proteins were subsequently chromatographed over another Ni^{++}-NTA column to remove the cleaved hexahistidine tags.

Purification of Hbp2 (Lmo2185)

E. coli BL21 containing pET28a encoding *lmo2185* was grown in LB broth at 37 °C until O.D.600 nm = 0.5. IPTG was added to 1 mM and the culture was harvested after 3 h. The cells were harvested by centrifugation at 10,000 × g for 15 min; the pellets were weighed and resuspended in a volume of lysis buffer (50 mM NaPi, 2 mM DTT, 3 mg DNase, 3 mg RNase, and a cocktail of protease inhibitors) that was 5 times their wet weight (g). The cell suspension was passed through the French Press twice at 14000 psi, and centrifuged at 10,000 × g for 15 min to remove debris and unbroken cells. The supernatant was collected and centrifuged at 100,000 × g for 1 hour to remove the cell envelope fraction. The supernatant was dialyzed twice against 4L of column buffer (50 mM NaPi, 300 mM NaCl, and 5 mM imidazole, pH 7.4), and loaded onto a column of cobalt-NTA sepharose (Talon Superflow; Pierce) equilibrated in the same buffer. The resin was washed with column buffer until absorbance at 280 nm reached background levels, and then further washed with steps of 20 mM and 40 mM imidazole in column buffer until the absorbance at 280 nm was not above background. His-tagged Hbp2 was eluted with 150 mM imidazole in column buffer. The protein was further purified by chromatography of its peak fractions (slightly

orange in color) over a Sephacryl S-100 size exclusion column (Pharmacia). Fractions containing purified, holo-6H-Hbp2 were combined and assayed to determine their protein concentration. The purified protein was boiled for 3 min in the presence of 0.5% SDS to remove bound Hn. The SDS and liberated Hn were removed by acetone precipitation: 9 volumes of ice cold acetone were added to the sample, which was incubated at −20 °C overnight, and pelleted by centrifugation at 16,000 × g for 30 min at 0 °C. The supernatant was immediately removed and the pellet was resuspended and renatured in TBS, pH 8.0, by incubation at RT for an hour or more. Purified, renatured 6H-Hbp2 was assayed for its ability to bind [^{59}Fe]-Hn. We attempted to remove its hexahistidine residues by thrombin cleavage, but we did not observe an alteration of its mobility in SDS-PAGE gels, suggesting that the 6H tag was resistant to cleavage. Nevertheless, the hexahistidine residues did not affect the affinity of either FhuD or HupD for Hn (*vide infra*).

Measurements of ferric siderophore and Hn binding

The affinities of 6H-FhuD, FhuD, 6HHupD and HupD for ferric siderophores and Hn were determined by intrinsic fluorescence quenching, using an SLM-AMINCO 8000 fluorimeter (Rochester, NY) upgraded to 8100 functionality. 20 nM FhuD or 33 nM apo-HupD in 3 mL TBS was added to a quartz cuvette and the fluorescence was recorded from 320 nm to 340 nm. Using constant agitation from a small stir bar, various concentrations of ferric siderophores or Hn (in DMSO) were added to the solutions of binding proteins and fluorescence was recorded after each addition. The background fluorescence (various concentrations of ferric siderophores or Hn in TBS) and volume changes were accounted for and the data were analyzed with the bound versus total function of GraFit 6.0 (Erithacus Software Ltd., Middlesex, UK) to determine the affinities (K_D values) of the binding proteins for the various iron complexes.

Determination of virulence in the mouse model system

Bacteria were grown, prepared and intravenously inoculated into pathogen-free, female Swiss mice (Janvier, Le Genest St. Isle, France), as previously described (Jin *et al.*, 2005). Bacteria were grown for 18 h in BHI broth, centrifuged, appropriately diluted in 0.15 M NaCl, and inoculated (0.5 ml) intravenously (i.v.) into mice via the lateral tail veins. Groups of five mice were challenged i.v. with various doses of bacteria, and mortality was monitored for 10 days. The virulence of the strains was estimated by the LD_{50} using the graphic probit method (Roth, 1961).

Intracellular multiplication

Bone marrow-derived macrophages from a BALB/c mouse were obtained and cultured (de Chastellier & Berche, 1994), and invasion assays were carried out essentially as previously described (Bigot *et al.*, 2005). Cell monolayers were incubated for 30 min at 37°C with the bacterial suspensions in Dulbecco modified Eagle medium (multiplicities of infection, 0.1) to allow penetration of the bacteria. After washing (t= 0 in the kinetic analysis), the cells were incubated for several hours in fresh culture medium containing gentamycin (50 ug/mL) to kill extracellular bacteria. At several points cells were washed three times in RPMI and processed for counting of infecting bacteria. The cells were lysed with distilled water, and the titer of viable bacteria released from the infected cells was determined by spreading dilutions onto BHI medium plates. The assays were performed in triplicate for each strain and time point.

Supplementary Material

Refer to Web version on PubMed Central for supplementary material.

Acknowledgments

The research was supported by NIH GM53836 and NSF MCB0417694 to PEK and SMN, and by CNRS, INSERM, and Université Paris Descartes as grants to AC, PEK and SMCN.

References

Annamalai R, Jin B, Cao Z, Newton SM, Klebba PE. Recognition of ferric catecholates by FepA. J Bacteriol. 2004; 186:3578–3589. [PubMed: 15150246]

Arnoux P, Haser R, Izadi N, Lecroisey A, Delepierre M, Wandersman C, Czjzek M. The crystal structure of HasA, a hemophore secreted by Serratia marcescens. Nat Struct Biol. 1999; 6:516–520. [PubMed: 10360351]

Arslan SY, Leung KP, Wu CD. The effect of lactoferrin on oral bacterial attachment. Oral Microbiol Immunol. 2009; 24:411–416. [PubMed: 19702956]

Asher C, de Villiers KA, et al. Speciation of ferriprotoporphyrin IX in aqueous and mixed aqueous solution is controlled by solvent identity, pH, and salt concentration. Inorg Chem. 2009; 48:7994–8003. [PubMed: 19572726]

Babusiak M, Man P, Sutak R, Petrak J, Vyoral D. Identification of heme binding protein complexes in murine erythroleukemic cells: study by a novel two-dimensional native separation -- liquid chromatography and electrophoresis. Proteomics. 2005; 5:340–350. [PubMed: 15627969]

Baichoo N, Wang T, et al. Global analysis of the Bacillus subtilis Fur regulon and the iron starvation stimulon. Mol Microbiol. 2002; 45(6):1613–1629. [PubMed: 12354229]

Bierne H, Garandeau C, Pucciarelli MG, Sabet C, Newton SM, del Portillo FG, Cossart P, Charbit A. Sortase B, a new class of sortase in Listeria monocytogenes. J. Bacteriol. 2004; 186:1972–1982. [PubMed: 15028680]

Bierne H, Mazmanian SK, Trost M, Pucciarelli MG, Liu G, Dehoux P, Jansch L, Garcia-del Portillo F, Schneewind O, Cossart P. Inactivation of the srtA gene in Listeria monocytogenes inhibits anchoring of surface proteins and affects virulence. Mol Microbiol. 2002; 43:869–881. [PubMed: 11929538]

Bigot A, Pagniez H, Botton E, Frehel C, Dubail I, Jacquet C, Charbit A, Raynaud C. Role of FliF and FliI of Listeria monocytogenes in flagellar assembly and pathogenicity. Infect Immun. 2005; 73:5530–5539. [PubMed: 16113269]

Braun V. Bacterial iron transport related to virulence. Contrib Microbiol. 2005; 12:210–233. [PubMed: 15496782]

Burkhard KA, Wilks A. Functional characterization of the Shigella dysenteriae heme ABC transporter. Biochemistry. 2008; 47:7977–7979. [PubMed: 18616281]

Cabrera G, Xiong A, Uebel M, Singh VK, Jayaswal RK. Molecular characterization of the iron-hydroxamate uptake system in Staphylococcus aureus. Appl Environ Microbiol. 2001; 67:1001–1003. [PubMed: 11157278]

Camejo A, Buchrieser C, Couve E, Carvalho F, Reis O, Ferreira P, Sousa S, Cossart P, Cabanes D. In vivo transcriptional profiling of Listeria monocytogenes and mutagenesis identify new virulence factors involved in infection. PLoS Pathog. 2009; 5:e1000449. [PubMed: 19478867]

Carniel E. The Yersinia high-pathogenicity island: an iron-uptake island. Microbes Infect. 2001; 3:561–569. [PubMed: 11418330]

Chastanet A, Derre I, Nair S, Msadek T. *clpB*, a novel member of the Listeria monocytogenes CtsR regulon, is involved in virulence but not in general stress tolerance. J. Bacteriol. 2004; 186:1165–1174. [PubMed: 14762012]

Clarke TE, Braun V, Winkelmann G, Tari LW, Vogel HJ. X-ray crystallographic structures of the Escherichia coli periplasmic protein FhuD bound to hydroxamate-type siderophores and the antibiotic albomycin. J Biol Chem. 2002; 277:13966–13972. [PubMed: 11805094]

Collier GS, Pratt JM, De Wet CR, Tshabalala CF. Studies on haemin in dimethyl sulphoxide/water mixtures. Biochem J. 1979; 179:281–289. [PubMed: 486081]

Dale SE, Sebulsky MT, Heinrichs DE. Involvement of SirABC in iron-siderophore import in Staphylococcus aureus. J Bacteriol. 2004; 186:8356–8362. [PubMed: 15576785]

de Chastellier C, Berche P. Fate of Listeria monocytogenes in murine macrophages: evidence for simultaneous killing and survival of intracellular bacteria. Infect Immun. 1994; 62:543–553. [PubMed: 8300212]

Demchick P, Koch AL. The permeability of the wall fabric of Escherichia coli and Bacillus subtilis. J Bacteriol. 1996; 178:768–773. [PubMed: 8550511]

de Villiers KA, Kaschula CH, et al. Speciation and structure of ferriprotoporphyrin IX in aqueous solution: spectroscopic and diffusion measurements demonstrate dimerization, but not μ-oxo dimer formation. J Biol Inorg Chem. 2007; 12:101–117. [PubMed: 16972088]

Dower WJ, Miller JF, Ragsdale CW. High efficiency transformation of E. coli by high voltage electroporation. Nucleic Acids Res. 1988; 16:6127–6145. [PubMed: 3041370]

Drazek ES, Hammack CA, Schmitt MP. Corynebacterium diphtheriae genes required for acquisition of iron from haemin and Hb are homologous to ABC haemin transporters. Mol Microbiol. 2000; 36:68–84. [PubMed: 10760164]

Emery T. Role of ferrichrome as a ferric ionophore in Ustilago sphaerogena. Biochemistry. 1971; 10:1483–1488. [PubMed: 5580666]

Falk, JE. Porphyrins and Metalloporphyrins. New York: American Elsevier Publishing Company, Inc; 1964.

Ginalski K. Comparative modeling for protein structure prediction. Curr Opin Struct Biol. 2006; 16:172–177. [PubMed: 16510277]

Glaser P, Frangeul L, Buchrieser C, Rusniok C, Amend A, Baquero F, Berche P, Bloecker H, Brandt P, Chakraborty T, Charbit A, Chetouani F, Couve E, de Daruvar A, Dehoux P, Domann E, Dominguez-Bernal G, Duchaud E, Durant L, Dussurget O, Entian KD, Fsihi H, Garcia-del Portillo F, Garrido P, Gautier L, Goebel W, Gomez-Lopez N, Hain T, Hauf J, Jackson D, Jones LM, Kaerst U, Kreft J, Kuhn M, Kunst F, Kurapkat G, Madueno E, Maitournam A, Vicente JM, Ng E, Nedjari H, Nordsiek G, Novella S, de Pablos B, Perez-Diaz JC, Purcell R, Remmel B, Rose M, Schlueter T, Simoes N, Tierrez A, Vazquez-Boland JA, Voss H, Wehland J, Cossart P. Comparative genomics of Listeria species. Science. 2001; 294:849–852. [PubMed: 11679669]

Grigg JC, Ukpabi G, Gaudin CF, Murphy ME. Structural biology of heme binding in the Staphylococcus aureus Isd system. J Inorg Biochem. 2010; 104:341–348. [PubMed: 19853304]

Hanahan D. Studies on transformation of Escherichia coli with plasmids. J Mol Biol. 1983; 166:557–580. [PubMed: 6345791]

Hanks TS, Liu M, McClure MJ, Lei B. ABC transporter FtsABCD of Streptococcus pyogenes mediates uptake of ferric ferrichrome. BMC Microbiol. 2005; 5:62. [PubMed: 16225685]

Immenschuh S, Baumgart-Vogt E, Mueller S. Heme Oxygenase-1 and Iron in Liver Inflammation: a Complex Alliance. Curr Drug Targets. 2010

Jin B, Newton SM, Shao Y, Jiang X, Charbit A, Klebba PE. Iron acquisition systems for ferric hydroxamates, haemin and haemoglobin in Listeria monocytogenes. Mol Microbiol. 2005; 59:1185–1198. [PubMed: 16430693]

Konopka K, Bindereif A, Neilands JB. Aerobactin-mediated utilization of transferrin iron. Biochemistry. 1982; 21:6503–6508. [PubMed: 6295467]

Konopka K, Mareschal JC, Crichton RR. Iron transfer form transferrin to ferritin mediated by polyphosphate compounds. Biochim Biophys Acta. 1981; 677:417–423. [PubMed: 6271255]

Kryshtafovych A, Venclovas C, Fidelis K, Moult J. Progress over the first decade of CASP experiments. Proteins. 2005; 61 Suppl 7:225–236. [PubMed: 16187365]

Lauer P, Chow MY, Loessner MJ, Portnoy DA, Calendar R. Construction, characterization, and use of two Listeria monocytogenes site-specific phage integration vectors. J Bacteriol. 2002; 184:4177–4186. [PubMed: 12107135]

Ledala N, Sengupta M, et al. Transcriptomic response of Listeria monocytogenes to iron limitation and Fur mutation. Appl Environ Microbiol. 2010; 76:406–416. [PubMed: 19933349]

Lei B, Liu M, Voyich JM, Prater CI, Kala SV, DeLeo FR, Musser JM. Identification and characterization of HtsA, a second heme-binding protein made by Streptococcus pyogenes. Infect Immun. 2003; 71:5962–5969. [PubMed: 14500516]

Lei B, Smoot LM, Menning HM, Voyich JM, Kala SV, Deleo FR, Reid SD, Musser JM. Identification and characterization of a novel heme-associated cell surface protein made by Streptococcus pyogenes. Infect Immun. 2002; 70:4494–4500. [PubMed: 12117961]

Li XL, Robbins JW Jr, Taylor KB. The production of recombinant beta-galactosidase in Escherichia coli in yeast extract enriched medium. J Ind Microbiol. 1990; 5:85–93. [PubMed: 1367464]

Liu M, Lei B. Heme transfer from streptococcal cell surface protein Shp to HtsA of transporter HtsABC. Infect Immun. 2005; 73:5086–5092. [PubMed: 16041024]

Maresso AW, Chapa TJ, Schneewind O. Surface protein IsdC and Sortase B are required for heme-iron scavenging of Bacillus anthracis. J Bacteriol. 2006; 188:8145–8152. [PubMed: 17012401]

Mazmanian SK, Skaar EP, Gaspar AH, Humayun M, Gornicki P, Jelenska J, Joachmiak A, Missiakas DM, Schneewind O. Passage of heme-iron across the envelope of Staphylococcus aureus. Science. 2003; 299:906–909. [PubMed: 12574635]

Mazmanian SK, Ton-That H, Su K, Schneewind O. An iron-regulated sortase anchors a class of surface protein during Staphylococcus aureus pathogenesis. Proc Natl Acad Sci U S A. 2002; 99:2293–2298. [PubMed: 11830639]

Meroueh SO, Bencze KZ, Hesek D, Lee M, Fisher JF, Stemmler TL, Mobashery S. Three-dimensional structure of the bacterial cell wall peptidoglycan. Proc Natl Acad Sci U S A. 2006; 103:4404–4409. Epub 2006 Mar 4409. [PubMed: 16537437]

Neidhardt FC, Bloch PL, Smith DF. Culture medium for enterobacteria. J Bacteriol. 1974; 119:736–747. [PubMed: 4604283]

Neilands, JB. Iron and its role in microbial physiology. In: Neilands, JB., editor. Microbial Iron Metabolism - A Comprehensive Treatise. New York: Academic Press; 1974. p. 4-34.

Newton SM, Igo JD, Scott DC, Klebba PE. Effect of loop deletions on the binding and transport of ferric enterobactin by FepA. Mol Microbiol. 1999; 32:1153–1165. [PubMed: 10383757]

Newton SM, Klebba PE, Raynaud C, Shao Y, Jiang X, Dubail I, Archer C, Frehel C, Charbit A. The svpA-srtB locus of Listeria monocytogenes: Fur-mediated iron regulation and effect on virulence. Mol Microbiol. 2005; 55:927–940. [PubMed: 15661014]

Newton SM, Trinh V, Pi H, Klebba PE. Direct measurements of the outer membrane stage of ferric enterobactin transport: postuptake binding. J Biol Chem. 2010; 285:17488–17497. [PubMed: 20335169]

Nygaard TK, Blouin GC, Liu M, Fukumura M, Olson JS, Fabian M, Dooley DM, Lei B. The mechanism of direct heme transfer from the streptococcal cell surface protein Shp to HtsA of the HtsABC transporter. J Biol Chem. 2006; 281:20761–20771. [PubMed: 16717094]

Perry RD, Shah J, Bearden SW, Thompson JM, Fetherston JD. Yersinia pestis TonB: role in iron, heme, and hemoprotein utilization. Infect Immun. 2003; 71:4159–4162. [PubMed: 12819108]

Premaratne RJ, Lin WJ, Johnson EA. Development of an improved chemically defined minimal medium for Listeria monocytogenes. Appl Environ Microbiol. 1991; 57:3046–3048. [PubMed: 1746963]

Ran Y, Liu M, Zhu H, Nygaard TK, Brown DE, Fabian M, Dooley DM, Lei B. Spectroscopic identification of heme axial ligands in HtsA that are involved in heme acquisition by Streptococcus pyogenes. Biochemistry. 2010; 49:2834–2842. [PubMed: 20180543]

Reeder BJ. The redox activity of hemoglobins: from physiologic functions to pathologic mechanisms. Antioxid Redox Signal. 2010; 13:1087–1123. [PubMed: 20170402]

Reniere ML, Torres VJ, Skaar EP. Intracellular metalloporphyrin metabolism in Staphylococcus aureus. Biometals. 2007; 20:333–345. [PubMed: 17387580]

Robinson SR, Dang TN, Dringen R, Bishop GM. Hemin toxicity: a preventable source of brain damage following hemorrhagic stroke. Redox Rep. 2009; 14:228–235. [PubMed: 20003707]

Roth Z. A graphic probit method for the calculation of LD50 and relative toxicity. Cesk Fysiol. 1961; 10:408–422. [PubMed: 14494411]

Schneider R, Hantke K. Iron-hydroxamate uptake systems in Bacillus subtilis: identification of a lipoprotein as part of a binding protein-dependent transport system. Mol Microbiol. 1993; 8:111–121. [PubMed: 8388528]

Schneider S, Paoli M. Crystallization and preliminary X-ray diffraction analysis of the haem-binding protein HemS from Yersinia enterocolitica. Acta Crystallogr Sect F Struct Biol Cryst Commun. 2005; 61:802–805.

Scott DC, Cao Z, Qi Z, Bauler M, Igo JD, Newton SM, Klebba PE. Exchangeability of N termini in the ligand-gated porins of Escherichia coli. J Biol Chem. 2001; 276:13025–13033. [PubMed: 11278876]

Sebulsky MT, Hohnstein D, Hunter MD, Heinrichs DE. Identification and characterization of a membrane permease involved in iron-hydroxamate transport in Staphylococcus aureus. J Bacteriol. 2000; 182:4394–4400. [PubMed: 10913070]

Sinclair, PR.; Gorman, N.; Jacobs, JM. Current Protocols in Toxicology. San Francisco: John Wiley and Sons, Inc.; 1999.

Singh A, Isaac AO, Luo X, Mohan ML, Cohen ML, Chen F, Kong Q, Bartz J, Singh N. Abnormal brain iron homeostasis in human and animal prion disorders. PLoS Pathog. 2009; 5:e1000336. [PubMed: 19283067]

Skaar EP, Humayun M, Bae T, DeBord KL, Schneewind O, Gaspar AH. Iron-source preference of Staphylococcus aureus infections. Science. 2004; 305:1626–1628. [PubMed: 15361626]

Smith K, Youngman P. Use of a new integrational vector to investigate compartment-specific expression of the Bacillus subtilis spoIIM gene. Biochimie. 1992; 74:705–711. [PubMed: 1391050]

Stauff DL, Skaar EP. The heme sensor system of Staphylococcus aureus. Contrib Microbiol. 2009; 16:120–135. [PubMed: 19494582]

Stojiljkovic I, Hantke K. Transport of haemin across the cytoplasmic membrane through a haemin-specific periplasmic binding-protein-dependent transport system in Yersinia enterocolitica. Mol Microbiol. 1994; 13:719–732. [PubMed: 7997183]

Stork M, Di Lorenzo M, Mourino S, Osorio CR, Lemos ML, Crosa JH. Two tonB systems function in iron transport in Vibrio anguillarum, but only one is essential for virulence. Infect Immun. 2004; 72:7326–7329. [PubMed: 15557661]

Tarlovsky Y, Fabian M, Solomaha E, Honsa E, Olson JS, Maresso AW. A Bacillus anthracis S-layer homology protein that binds heme and mediates heme delivery to IsdC. J Bacteriol. 2010; 192:3503–3511. [PubMed: 20435727]

Thompson JM, Jones HA, Perry RD. Molecular characterization of the hemin uptake locus (hmu) from Yersinia pestis and analysis of hmu mutants for hemin and hemoprotein utilization. Infect Immun. 1999; 67:3879–3892. [PubMed: 10417152]

Tidmarsh GF, Klebba PE, Rosenberg LT. Rapid release of iron from ferritin by siderophores. J Inorg Biochem. 1983; 18:161–168. [PubMed: 6222161]

Toledo-Arana A, Dussurget O, Nikitas G, Sesto N, Guet-Revillet H, Balestrino D, Loh E, Gripenland J, Tiensuu T, Vaitkevicius K, Barthelemy M, Vergassola M, Nahori MA, Soubigou G, Regnault B, Coppee JY, Lecuit M, Johansson J, Cossart P. The Listeria transcriptional landscape from saprophytism to virulence. Nature. 2009; 459:950–956. [PubMed: 19448609]

Tong Y, Guo M. Cloning and characterization of a novel periplasmic heme-transport protein from the human pathogen Pseudomonas aeruginosa. J Biol Inorg Chem. 2007; 12:735–750. [PubMed: 17387526]

Touhami A, Jericho MH, Beveridge TJ. Atomic force microscopy of cell growth and division in Staphylococcus aureus. J Bacteriol. 2004; 186:3286–3295. [PubMed: 15150213]

Tsai HN, Hodgson DA. Development of a synthetic minimal medium for Listeria monocytogenes. Appl Environ Microbiol. 2003; 69:6943–6945. [PubMed: 14602660]

Wayne R, Frick K, Neilands JB. Siderophore protection against colicins M, B, V, and Ia in Escherichia coli. J Bacteriol. 1976; 126:7–12. [PubMed: 131121]

Wyckoff EE, Schmitt M, Wilks A, Payne SM. HutZ is required for efficient heme utilization in Vibrio cholerae. J Bacteriol. 2004; 186:4142–4151. [PubMed: 15205415]

Zhao S, Montanez GE, Kumar P, Sannigrahi S, Tzeng YL. Regulatory role of the MisR/S two-component system in hemoglobin utilization in Neisseria meningitidis. Infect Immun. 2010; 78:1109–1122. [PubMed: 20008531]

Zhu H, Xie G, Liu M, Olson JS, Fabian M, Dooley DM, Lei B. Pathway for heme uptake from human methemoglobin by the iron-regulated surface determinants system of Staphylococcus aureus. J Biol Chem. 2008; 283:18450–18460. [PubMed: 18467329]

Zhu H, Liu M, Lei B. The surface protein Shr of Streptococcus pyogenes binds heme and transfers it to the streptococcal heme-binding protein Shp. BMC Microbiol. 2008; 8:15. [PubMed: 18215300]

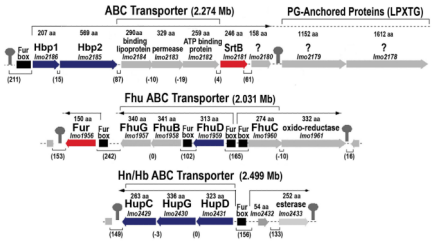

Figure 1. Chromosomal loci

A schematic representation of the *srtB, fhu* and *hup* regions of the *L. monocytogenes* chromosome shows loci involved in iron acquisition (red and blue genes are considered in this report). The *srtB* region (2.274 Mb) contains genes for secreted, peptidoglycan-associated proteins (*lmo2185*, 6), the sortase (*srtB*) that anchors them to the cell wall, a putative ABC-transporter (*lmo2182–2184*) and two SrtA-dependent cell wall proteins (*lmo2178, 2179*) (Bierne, 2004, Newton *et al.*, 2005). The *fhu* region (2.031 Mb) encodes a substrate binding lipoprotein (FhuD) and a putative ferric hydroxamate ABC-transporter (FhuBCG) (Jin *et al.*, 2005). The *hupDGC* locus (2.499 Mb) encodes a substrate binding lipoprotein (HupD) and a putative ABC transporter for Hn/Hb (Jin *et al.*, 2005). Parenthetic values refer to the distance (bp) between adjacent genes.

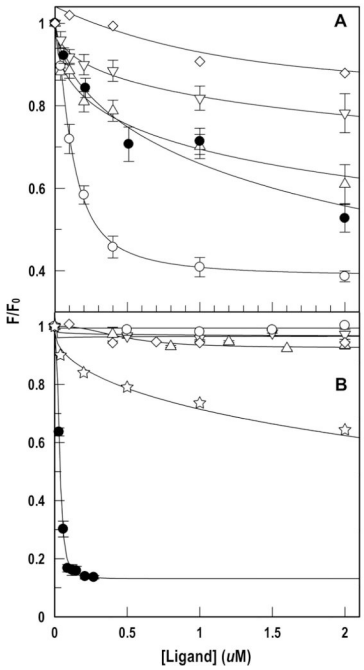

Figure 2. Fluorescence spectroscopic comparison of FhuD and HupD binding specificities

L. monocytogenes 6H-FhuD and 6H-HupD were purified by affinity chromatography on Ni^{++}-NTA agarose and tested for their ability to bind ferric siderophores and Hn, by monitoring quenching of intrinsic Trp fluorescence. **(Top panel)** FhuD, the ferric hydroxamate binding protein, recognized a variety of iron complexes, including Hn, whereas **(bottom panel)** HupD was specific for its only ligand, Hn [(A) ferrioxamine B (FxB); (X) ferrichrome (Fc); (Δ) ferrichrome A (FcA); (E) ferric enterobactin (FeEnt); (α) haemin (Hn); (ϑ) protoporphyrin IX (PPIX)]. Removal of their 6H tags (by cleavage with thrombin) had no effect on the specificities or affinities of the binding proteins (Table 1).

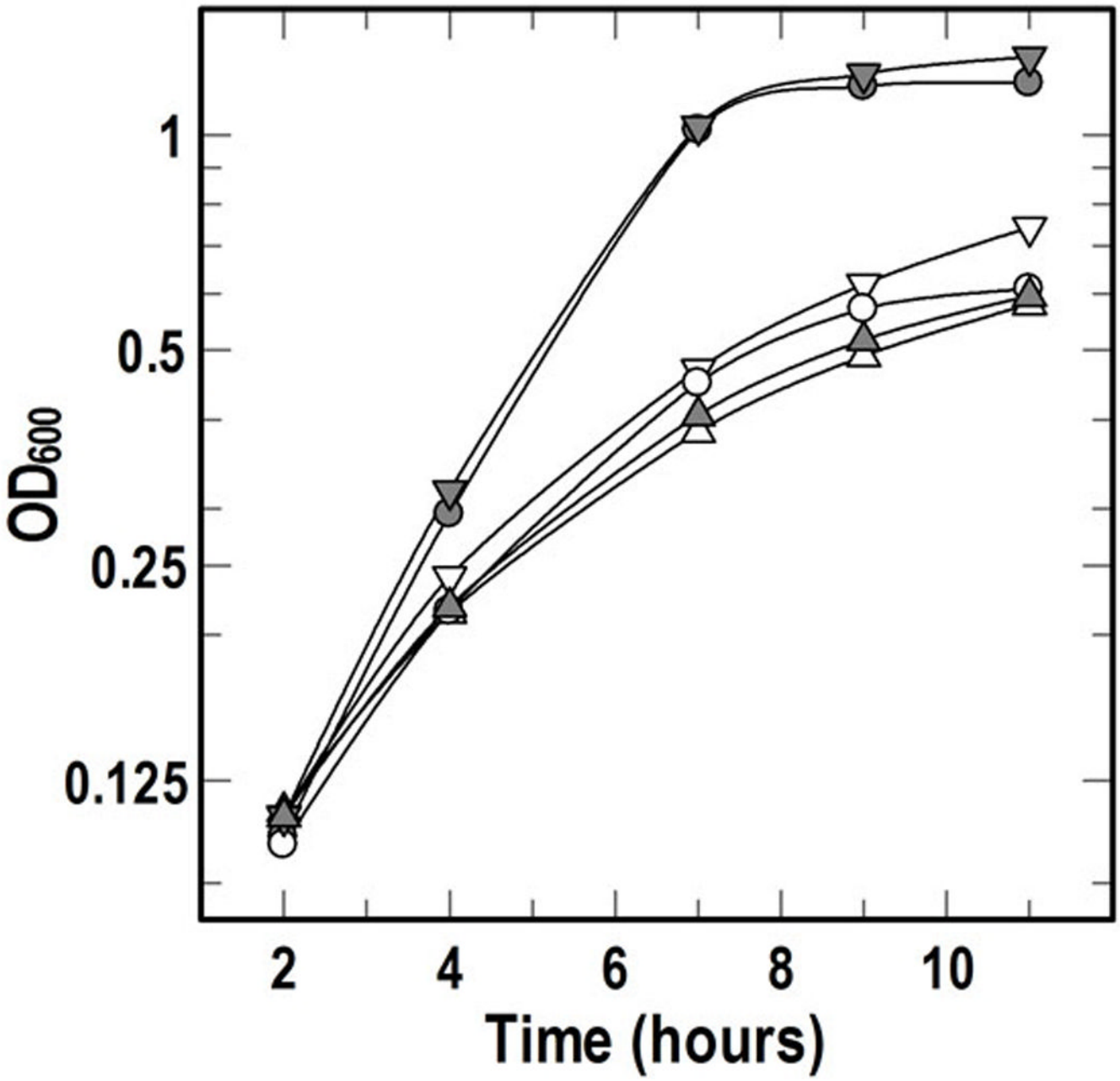

Figure 3. Growth of mutants in BHI with 2, 2'-bipyridyl

Cells were grown in BHI overnight, and 2.5×10^7 cells were subcultured into BHI containing 1 mM 2, 2'-bipyridyl. After 2 hours, Hn (2 mM in 40% DMSO) was diluted into the media to 0.2 μM. Growth curves defined by open symbols derive from parent cultures to which no Hn was added; curves from filled symbols represent data derived from cultures to which 0.2 μM Hn was added: (A) EGD-e, (X) ΔHupG, (Δ) ΔHupG_pPL2*hupG*$^+$. For clarity, equivalent results with EGD-e derivatives carrying *ΔhupC* or *ΔhupDGC* are not shown. The plotted data represent a single experiment, but the experiment was repeated at least 3 times with the same results.

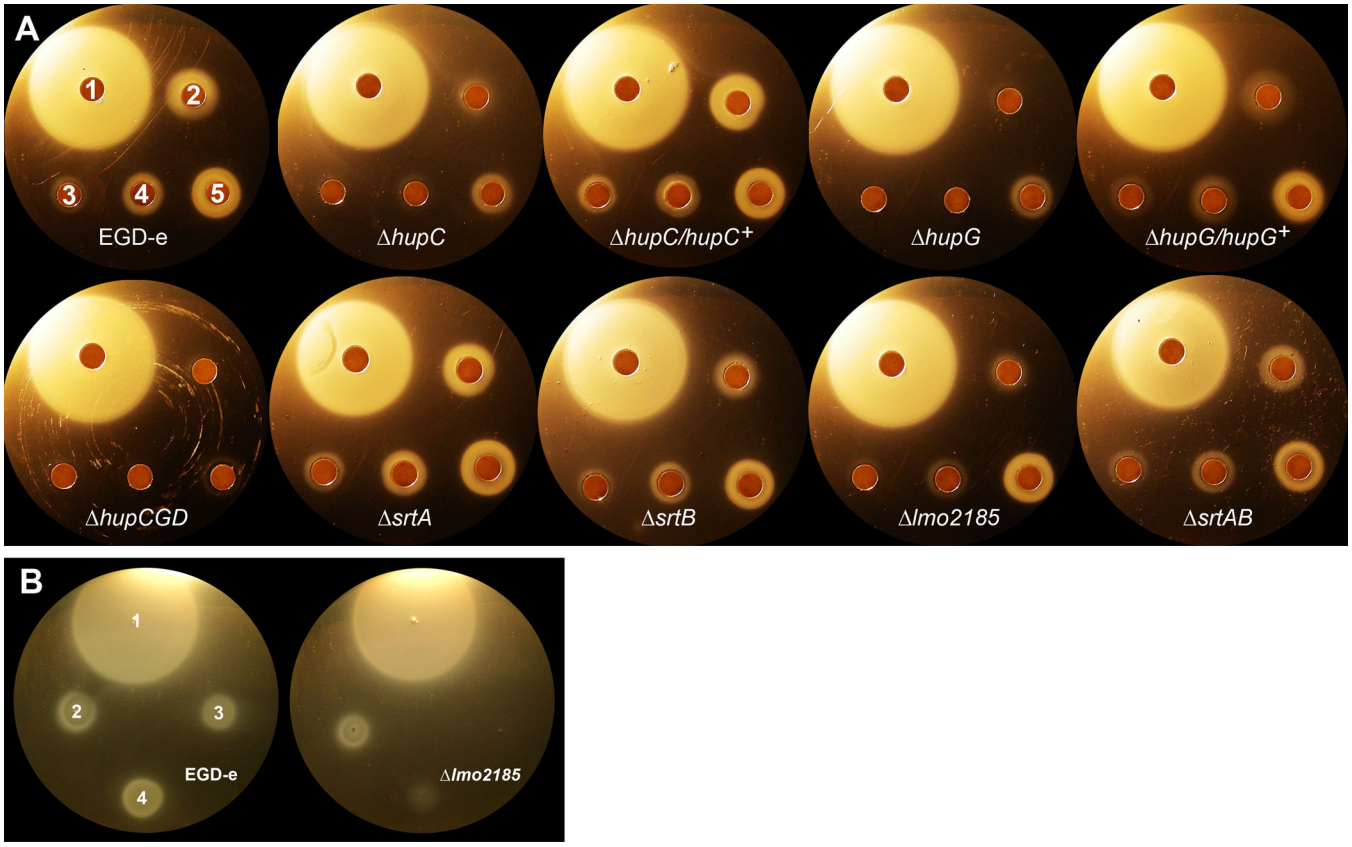

Figure 4. Iron nutrition tests of *L. monocytogenes* strains

EGD-e and its mutants were grown in BHI, subjected to iron deprivation at mid-log by addition of 1 mM bipyridyl, and plated on BHI agar containing 0.25 mM bipyridyl (Newton *et al*., 2005). **(A) Hn/Hb utilization.** Paper discs were placed on the agar, and 10μl aliquots of different iron compounds were applied to the discs: (1) 50 uM Fc; (2) 15 μM Hb; (3–5) 0.5 μM, 5 μM and 50 μM Hn, respectively. Mutants in the *hup* operon had reduced iron supply from Hn and Hb, whereas sortase mutants and *Δlmo2185* showed little reduction in this assay. All the strains normally utilized the hydroxamate siderophore Fc. **(B) Utilization of iron from purified Lmo2185.** 10μl aliquots of compounds were applied with a micropipette tip directly to the agar: (1) 50 uM Fc; (2) 0.5 μM Hn; (3) 10.5 uM apo-Lmo2185; (4) partially saturated Lmo2185 (1.6 uM Lmo2185 containing 0.7 uM Hn). Both apo- and holo-Lmo2185 supplied iron to EGD-e, but not to its *Δlmo2185* derivative.

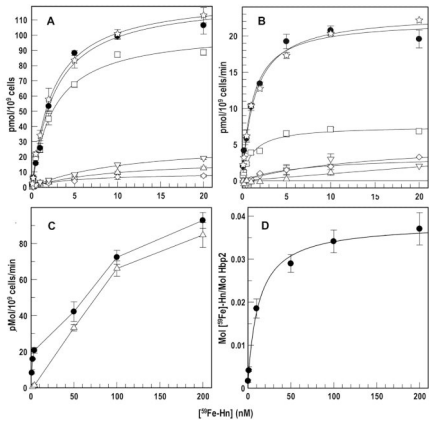

Figure 5. Hn binding and transport by EGD-e and its derivatives

In panels A–C, wild type strain EGD-e (α), or its derivatives carrying the individual mutations *Δhup* (□); *ΔsrtA* (ϑ), *ΔsrtB* (Δ), *ΔsrtA*B (E) and *Δlmo2185* (X) were grown in BHI, subcultured twice in MOPS-L, and tested for their ability to bind or transport [^{59}Fe]-Hn (Jin *et al.*, 2005). Binding (A) and transport (B) assays revealed impaired Hn acquisition by *Δhup*, *ΔsrtB*, and *Δlmo2185* at low nanomolar concentrations of the iron porphyrin, but no effect of *Δlmo2185* at Hn concentrations ≥ 50 nM (C). In panel D, purified Lmo2185 was mixed with increasing concentrations of [^{59}Fe]-Hn and the protein was collected on filters, which were washed and counted to determine the amount of Hn bound (Experimental Procedures). The experiments were repeated 3 or 4 times; bars on the data points represent standard deviations of the mean values. In panel A, from the 6 fitted curves (bound *vs* total) the mean standard deviation was 6.7% for K_D values and 22.3% for capacity; in panel B, from the 5 fitted curves (enzyme kinetics) the mean standard deviatiion was 8.5% for K_M values and 20.7% for V_{max}; In panel D, from the fitted curve (bound *vs* total) the mean standard deviation was 4.1% for the K_D value and 18.7% for capacity.

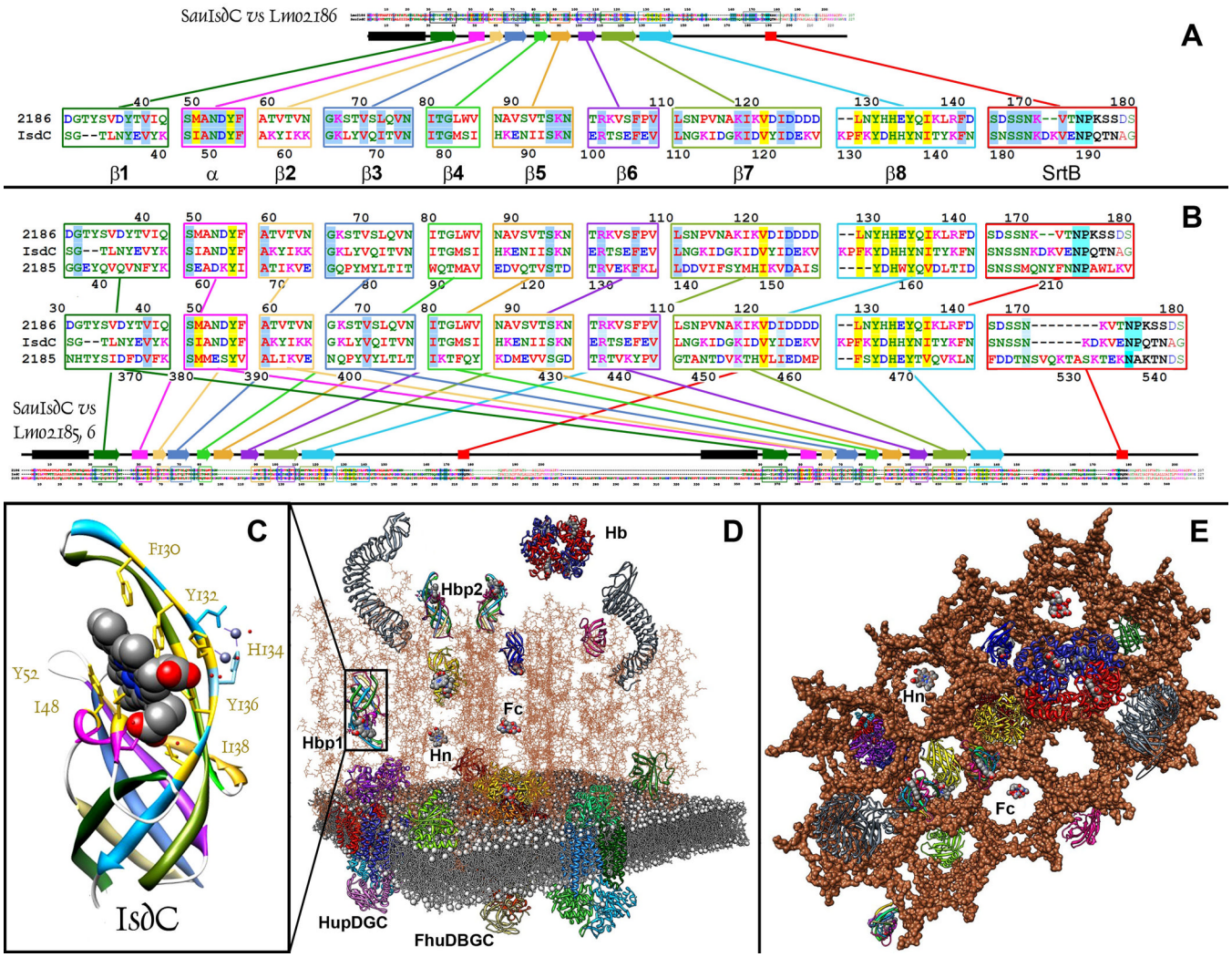

Figure 6. Sequence, structural and potential spatial relationships of heme binding proteins in the Gram-positive cell envelope

A. Lmo2186 (Hbp1) and SauIsdC The sequences of LmoHbp1 and SauIsdC are 30% identical overall (69 of 227 residues), confirming their structural relatedness. The foundation of their conservation is in α and β secondary structure [the colored boxes in panels A and B correlate with the depiction of SauIsdC crystal structure (2O6P) in panel C]: in the α and β elements the extent of sequence identity is 78%. **B. Lmo2185 (Hbp2), LmoHbp1 and SauIsdC.** LmoHbp2 comprises a duplication of LmoHbp1, separated by ~200 amino acids (residues 163 – 351) in the middle of the protein. Its N-terminal half (a.a. 1 – 219) has 21% (43 of 207 residues) and 23% (51 of 227 residues) overall identity to LmoHbp1 and SauIsdC, respectively. The main sequence diversity occurs in loops and turns; in the α and β elements the extent of identity is 48% and 59%, respectively. Its C-terminal half (a.a. 352–569) has 25% (52 of 207 residues) and 22% (50 of 227 residues) overall identity to LmoHbp1 and SauIsdC, with 58% and 57% identity in α and β structure, respectively. **C. SauIsdC.** Eight residues its single α-helix and β-strands 7 and 8 complex heme in SauIsdC (2O6P). Theses amino acids in IsdC (yellow) are identical or conservatively substituted in Hbp1 and Hbp2 (both the N - and C - domains), including Y52 and Y132, which coordinate iron in the porphyrin ring. The only exception is I48 in IsdC, substituted by E59 in Hbp2. **D and E. Sortase-dependent and independent heme transport through the Gram-positive**

bacterial cell envelope. The cytoplasmic membrane (phospholipids in stick format; phosphate atoms in space filling form) contains transporters for iron compounds, such as the HupDGC and FhuDBGC putative ABC-transporters (shown in ribbon format). The PG polymer (shown in wire format in panel D, and as space filling surfaces in panel E) surrounds the cell as a series of conjoined hexagonal pores with approximately 70 Å diameter (coordinates through the courtesy of S. Mobashery; Meroueh *et al.* 2006). This architecture creates pathways for diffusion of small solutes, like ferric siderophores (Fc) or porphyrins (Hn), through the PG matrix (best viewed in E). At concentrations above 50 nM, Hn permeates the PG layer and directly adsorbs to lipoproteins of the ABC-transporters. On the other hand, sortases A and B attach haem binding proteins (for example, listerial Hbp1 and Hbp2) and other proteins to the cell wall matrix by peptide bonds to Lys or DAP in PG. The anchored proteins create a sortase-dependent pathway of Hn/Hb (Hb (PDB file 3HF4) uptake. At very low Hn concentrations Hbp1 and Hbp2 initiate transport by capturing the iron porphyrin from solution and subsequently transferring it to the underlying ABC transporters. In this cartoon Hbp1 and Hbp2 were modeled from their relationship to IsdC (2O6P); HupDGC and FhuDBGC were modeled from their relationship to the iron ABC transporter of *Haemophilus influenzae* (2NQ2) and the maltose ABC transporter of *E. coli* (3FH6), respectively. The molecules were rendered and assembled with Chimera (UCSF); high resolution images with more detailed explanations are provided as supplementary Fig. S4).

Table 1

Affinities of listerial proteins FhuD (Lmo1959) and HupD (Lmo2431) for iron chelates.

Iron Complex	Binding K_d[a]			
	FhuD-6H	**FhuD**	**HupD-6H**	**HupD**
Fc	523 ± 243	243 ± 13	NB[b]	ND[c]
FcA	497 ± 130	ND	NB	ND
FxB	123 ± 9.6	44 ± 3	NB	ND
FeEnt	2330 ± 678	ND	NB	ND
Hn	588 ± 79	711 ± 183	36 ± 11	26 ± 5
PPIX	276 ± 32	ND	1148	ND

[a]The data derive from repeated measurements (3–5 trials) of intrinsic fluorescence quenching (Fig. 2), from which we used Grafit 7.0.1 to calculate the binding K_d (nM) for each iron complex. The data are expressed as K_d ± the standard deviation of the mean values (the mean SD of all determinations was 20.2%). NB: no binding; ND: not determined

Table 2

Binding and transport properties of selected strains.

strain	Binding [a]		Transport [a]	
	K_d	Cap.	K_m [b]	V_{max} [b]
EGD-e	2.4 ± 0.47	129.5 ± 5.6	1.2 ± 0.2	22.2 ± 0.9
Δhup	2.5 ± 0.45	105 ± 4.2	1.1 ± 0.2	7.5 ± 0.3
ΔsrtA	2.3 ± 0.16	129 ± 1.9	1.4 ± .2	23.1 ± 0.6
ΔsrtB	9.9 ± 1.3	18.7 ± 0.9	7.1 ± 7.5	3.5 ± 1.6
ΔsrtAB	5.1 ± 3	9 ± 1.5	15.1 ± 6.4	5.6 ±1.3
Δ*lmo2185*	11.4 ± 2.6	30.1 ± 2.9	NS	NS

[a] The data derive from repeated measurements (3–5 trials) of [^{59}Fe]-Hn binding or transport (Fig. 5), from which we used Grafit 7.0.1 to calculate its binding K_d (nM) and capacity (Cap; pMol/10^9cells), and its transport K_M (nM) and V_{max} (pMol/10^9cells/min) in the different genetic backgrounds. The data are expressed as the measured parameter ± the standard deviation of the mean values (the mean SD for K_D, Cap, K_M and V_{max} were 23%, 7%, 39% and 16%, respectively).

[b] NS: non-saturation transport process

Table 3

LD_{50} of *L. monocytogenes* strains.

Strain	LD_{50}
EGD-e	$10^{4.5}$
ΔhupC	$10^{5.5}$
ΔhupG	$10^{5.7}$
ΔhupD	$10^{5.5}$
ΔhupDGC	$10^{6.4}$

Wild-type strain EGD-e and site-directed deletion mutants were evaluated in the mouse infection model, and LD_{50} values were determined by the probit graphic method (Roth, 1961).

Table 4

Gram-positive bacterial Hn/Hb and ferric siderophore binding and transport proteins.

Organism	Iron Complex	PG Binding Protein	CM permease	References
L. monocytogenes	Hn/Hb	Hbp1, Hbp2	HupDGC	This report
	FxB, Fc, FcA	none	FhuCDG	(Jin *et al.*, 2005)
B. subtilis/anthracis	Hn/Hb	IsdX1, IsdX2	ND	(Fabian *et al.*, 2009)
	Fc	none	FhuCDG	(Schneider & Hantke, 1993)
S. aureus	Hn/Hb	IsdA, B, C, H	IsdDEF, HtsABC	(Zhu *et al.*, 2008; Skaar *et al.*, 2004)
	Staphylobactin	none	SirABC	(Dale *et al.*, 2004)
	Fc, FxB,	none	FhuCBG	(Sebulsky *et al.*, 2000; Cabrera *et al.*, 2001)
S. pyogenes	Hn/Hb	Shr, Shp	HtsABC	(Lei et al., 2002; Zhu et al., 2008) (Liu & Lei, 2005, Nygaard *et al.*, 2006)
	Fc	none	FtsABCD	(Hanks *et al.*, 2005)

See the Discussion for an explanations of the various transport systems.

Table 5

Bacterial strains and plasmids

Strain/plasmid	Markers/Characteristics	Reference/source
Strains		
E. coli		
DH5α	*supE44 ΔlacU169(Φ80lacZ ΔM15) hsdR17 recA1 endA1 gyra96 thi-1 relA1*	(Hanahan, 1983)
SM10	*F–thi-1 thr-1 leuB6 recA tonA21 lacY1 supE44* (Mu_{C+}) λ^- Km^r Tra^+	(Lauer et al., 2002)
XL-1 blue	*recA1 endA1 gyrA96 thi-1 hsdR17 supE44 relA1 lac*	Stratagene
L. monocytogenes		
EGD-e	Wild-type strain	(Glaser et al., 2001)
ΔHupC	*ΔhupC*	(Jin et al., 2005)
ΔHupG	*ΔhupG*	This study
ΔHupD	*ΔhupD*	This study
ΔHup	*ΔhupC, ΔhupG, ΔhupD*	This study
ΔHupC.comp	*ΔhupC*, complemented by pPL2_$hupC^+$	This study
ΔhupG.comp	*ΔhupG*, complemented by pPL2_$hupG^+$	This study
ΔSrtA	*ΔsrtA*	(Bierne *et al.*, 2002)
ΔSrtB	*ΔsrtB*	(Bierne, 2004)
ΔSrtAB	*ΔsrtA, ΔsrtB*	Pascal Cossart
Δlmo2185	*Δlmo2185*	(Newton et al., 2005)
Plasmids		
pKSV7	*E. coli - L. monocytogenes* shuttle vector	(Smith & Youngman, 1992)
pPL2	site-specific shuttle integration vectors	(Lauer et al., 2002)
pPro	pPL2 harboring *hup* promotor	This study
pCHupC	pPL2 harboring *hup* promoter and *hupC*	This study
pCHupG	pPL2 harboring *hup* promoter and *hupG*	This study

Table 6

Components of iron-deficient media.

Component	Concentration in medium				
	KRM[a]	MWB[b]	HTM[c]	MOPS[d]	MOPS(L)
MOPS			100 mM	40 mM	40 mM
K_2HPO_4		48.2 mM	4.82 mM	1.32 mM	1.32 mM
NH_4Cl				9.52 mM	9.52 mM
$MgCl_2$				0.523 mM	0.523 mM
K_2SO_4				0.276 mM	0.276 mM
$CaCl_2$				5×10^{-4}mM	5×10^{-4}mM
NaCl				50 mM	50 mM
Na_2HPO_4		115.5 mM	11.55 mM		
$MgSO_4$		1.70 mM	1.70 mM		
KH_2PO_4					
$(NH4)_2SO_4$			0.6 mg/ml		
$NaHCO_3$	0.2%				
Ferric Citrate		360 μM			
Glucose	0.4%	0.99%	0.99%	0.4%	1.0%
RPMI1640	1.04%				
Thiamine	1.0 μg/ml	2.96 μM	2.96 μM		1.0 μg/ml
Riboflavin	0.5 μg/ml	1.33 μM	1.33 μM		0.5 μg/ml
Biotin	1.0 μg/ml	2.05 μM	2.05 μM		1.0 μg/ml
Lipoic acid	5×10^{-3}μg/ml	24.0 pM	24.0 pM		5×10^{-3}μg/ml
Histidine		0.1 mg/ml			
Tryptophan	0.05 mg/ml	0.1 mg/ml			0.05 mg/ml
Leucine		0.1 mg/ml			
Isoleucine		0.1 mg/ml			
Valine		0.1 mg/ml			
Arginine		0.1 mg/ml			

Component	Concentration in medium				
	KRM[a]	MWB[b]	HTM[c]	MOPS[d]	MOPS(L)
Cysteine		0.1 mg/ml	0.1 mg/ml		0.1 mg/ml
Methionine		0.1 mg/ml	0.1 mg/ml		
Glutamine		0.6 mg/ml			0.6 mg/ml
Casamino acids	0.1%				0.1%
Micronutrients	+			+	114.9

[a](Newton *et al.*, 2005)

[b](Premaratne *et al.*, 1991)

[c](Tsai & Hodgson, 2003)

[d](Neidhardt *et al.*, 1974)

[e]Micronutrients contain: $(NH_4)_6Mo_7O_{24}{\cdot}4H_2O$ (3×10^{-7} M),$CoCl_2{\cdot}6H_2O$ (3×10^{-6} M), HBO_3 (4×10^{-5} M), $CuSO_4{\cdot}5H_2O$ (10^{-6} M), $MnCl_2$ (8×10^{-6} M), $ZnCl_2$ (10^{-6} M).